

α -decaying states in $^{10,12}\text{Be}$ populated in the $^{10}\text{Be}(^{14}\text{C},^{10,12}\text{Be})$ reactionN. Curtis,^{1,*} N. I. Ashwood,¹ L. T. Baby,² T. D. Baldwin,³ T. R. Bloxham,¹ W. N. Catford,³ D. D. Caussyn,² M. Freer,¹
C. W. Harlin,³ P. McEwan,¹ D. L. Price,¹ D. Spingler,² and I. Wiedenhover²¹*School of Physics and Astronomy, University of Birmingham, Edgbaston, Birmingham B15 2TT, United Kingdom*²*Department of Physics, Florida State University, Tallahassee, Florida 32306-4350, USA*³*School of Electronics and Physical Sciences, University of Surrey, Guildford, Surrey GU2 7XH, United Kingdom*

(Received 7 February 2006; published 8 May 2006)

A search has been made for the $^6\text{He} + ^6\text{He}$ and $\alpha + ^8\text{He}$ decay of the molecular rotational band in ^{12}Be using the $^{10}\text{Be}(^{14}\text{C},^{12}\text{Be}^*)^{12}\text{C}$ reaction at 88.5 MeV. Although the $\alpha + ^6\text{He}$ decay of ^{10}Be was observed in the data set there is no evidence for the breakup of ^{12}Be . The cross-section upper limits for the $^{10}\text{Be}(^{14}\text{C},^6\text{He } ^6\text{He})^{12}\text{C}$ and $^{10}\text{Be}(^{14}\text{C},\alpha ^8\text{He})^{12}\text{C}$ reactions are 50 and 300 nb respectively.

DOI: [10.1103/PhysRevC.73.057301](https://doi.org/10.1103/PhysRevC.73.057301)

PACS number(s): 23.60.+e, 23.70.+j, 25.60.-t, 27.20.+n

In recent years a number of experiments have been performed to study the $^6\text{He} + ^6\text{He}$ molecular nature of ^{12}Be [1–4]. The first employed a 31.5 MeV/nucleon ^{12}Be beam to study the $p(^{12}\text{Be},^6\text{He } ^6\text{He})p$ reaction [1,2]. A number of discrete states were observed in ^{12}Be , and a study of the $^6\text{He} + ^6\text{He}$ fragment angular correlations allowed several tentative spin assignments to be made. The energy/spin systematics for the states indicate that a highly deformed rotational structure was populated in the reaction. The gradient of the rotational band (150 ± 40) keV, is consistent with that calculated for two touching ^6He nuclei in a molecular configuration (165 keV with $r_0 = 1.3$ fm) and very much lower than that predicted for a spherical ^{12}Be nucleus (360 keV). This work therefore provided evidence for a deformed $^6\text{He} + ^6\text{He}$ cluster structure in ^{12}Be , possibly linked to an α -4n- α molecule. More recently a 75 MeV/nucleon ^{14}Be beam and ^{12}C target was used [3] to study two neutron removal and provided evidence for a new state in ^{12}Be at 11.8 MeV for which a tentative spin assignment of 0^+ was made. This state appears to lie on the rotational band observed in Refs. [1,2], and was proposed as a band-head member of the $^6\text{He} + ^6\text{He}$ molecular band. In Ref. [4] a 60 MeV/nucleon ^{12}Be beam and a liquid helium target were used to study the $^4\text{He}(^{12}\text{Be},^6\text{He } ^6\text{He})^4\text{He}$ reaction. Two new states were reported at 10.9 and 11.3 MeV with spin assignments of 0^+ and 2^+ , respectively. These again appear to lie on the same rotational band as the previous states observed in Refs. [1–3].

In order to study the $^6\text{He} + ^6\text{He}$ and $\alpha + ^8\text{He}$ decay of ^{12}Be a measurement of the $^{10}\text{Be}(^{14}\text{C},^{12}\text{Be}^*)^{12}\text{C}$ reaction has been performed. The ^{14}C beam, available at higher intensity than a secondary fragmentation beam and with greater beam quality, should, in principle, allow a high resolution study of the ^{12}Be rotational band and provide sufficient statistics to allow firm spin assignments to be made. In addition, data on the $\alpha + ^6\text{He}$ decay of ^{10}Be was also collected.

The experiment was performed at the Florida State University superconducting LINAC facility. The ^{14}C beam was accelerated to ~ 90 MeV, the exact beam energy being

determined later during the offline data analysis (see below). The beam was not debunched following LINAC acceleration resulting in a beam energy spread of ~ 800 keV. The integrated beam exposure was 0.44 mC. The reaction target, $280 \mu\text{g}/\text{cm}^2$ BeO, was mounted on a $1.0 \text{ mg}/\text{cm}^2$ Pt backing for mechanical support. The ^{10}Be enrichment was $\sim 94\%$ [5] and the total ^{10}Be thickness $\sim 100 \mu\text{g}/\text{cm}^2$. The target was orientated with the Pt backing upstream and the BeO facing the detectors.

The He decay fragments were detected in coincidence in an array of two (50 mm \times 50 mm) detector telescopes. The first element in each telescope was a 65 μm thick silicon double sided strip detector (DSSD) used for energy loss (ΔE) measurements. Each DSSD was segmented into 32 independent (50 mm \times 3 mm) strips, with 16 horizontal strips on the front face and 16 vertical strips on the back face. The second element was a 500 μm thick silicon resistive strip detector (RSD). This was segmented into 16 independent horizontal (50 mm \times 3 mm) strips which were aligned with those on the front face of the DSSD detectors. Resistive charge division provided position information along the strip length with a resolution of ~ 0.3 mm. The vertical position resolution, ± 1.5 mm, was limited by the strip pitch. The energy resolution for 6.118 MeV α -particles obtained from a ^{252}Cf source was 115 keV. The third element in each telescope was a 10 mm thick CsI scintillator, used to stop energetic particles that passed through both silicon detectors. In combination the three detectors provided energy and position information as well as particle identification for all isotopes from ^1H to ^7Li . The two telescopes were positioned horizontally either side of the beam axis at center angles of 17° and at a target to RSD distance of 140 mm. In order to shield the detectors from beam particles elastically scattered from the Pt backing of the target 250 μm mylar sheets were placed in front of each telescope. These stopped the ^{14}C beam nuclei but allowed the He decay products to pass through to the detectors. The telescopes were calibrated using ^{241}Am , ^{244}Cm and ^{252}Cf α -particle sources and 23.9 and 42.5 MeV ^{12}C beams scattered from Au and C targets. Data were taken with the mylar absorbers both in place and removed to allow a determination of the thickness via a consideration of particle energy loss. The mylar thickness obtained by this method was $(255 \pm 5) \mu\text{m}$, consistent with the $(258 \pm 6) \mu\text{m}$ measured using a micrometer.

*E-mail: N.Curtis@bham.ac.uk

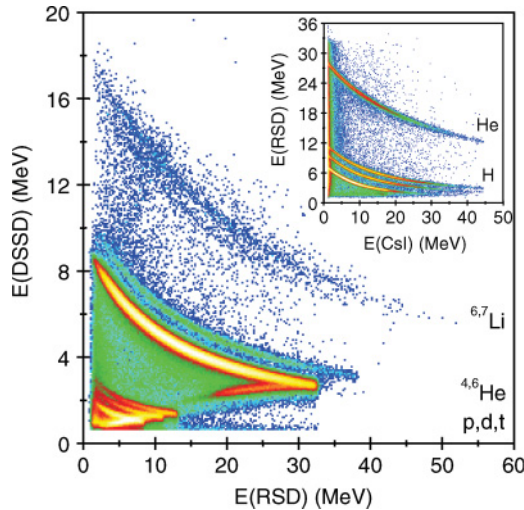


FIG. 1. (Color online) PI spectrum obtained using the DSSD and RSD detectors of a telescope. In the inset a PI using the RSD and CsI energies is shown.

The He fragments arising from the decay of excited states in Be were identified using the ΔE - E information provided by the detector telescopes. Figure 1 shows a particle identification (PI) spectrum obtained using the DSSD (ΔE) and RSD (E) detectors of one telescope. The isotopes $^{1,2,3}\text{H}$, $^{4,6}\text{He}$ and $^{6,7}\text{Li}$ are observed. There is little, if any, evidence, for ^8He . In the inset to Fig. 1 a second PI spectrum, obtained using the RSD energy (ΔE) and the CsI energy (E), is shown. These events correspond to those in which highly energetic particles, with sufficient energy to pass through both of the silicon detectors, were incident on the telescope. The isotopes $^{1,2,3}\text{H}$ and ^4He are clearly observed in this spectrum.

After PI selection a Q -value spectrum was produced for each reaction by summing the energy of the two detected fragments (E_1 and E_2) with that of the undetected recoil (E_{rec}). The total energy (E_{tot}) in the exit channel, $E_1 + E_2 + E_{\text{rec}}$, is equal to the sum of the beam energy and the three body Q -value for the reaction, $E_{\text{beam}} + Q_3$ [6]. The recoil energy was determined from the missing momentum between the beam and two detected particles and by making an assumption of the recoil mass. In Fig. 2 the E_{tot} spectrum for the $^{10}\text{Be}(^{14}\text{C},\alpha\ ^6\text{He})^{14}\text{C}$ reaction is shown. The peak labeled Q_{ggg} corresponds to events in which all three final state particles were emitted in the ground state. The centroid energy of this peak was used to determine the exact beam energy provided by the LINAC. The reconstructed position of the peak ($E_1 + E_2 + E_{\text{rec}}$) will only coincide with the predicted energy ($E_{\text{beam}} + Q_3$) if the beam energy used in the reconstruction is correct. By reconstructing the E_{tot} spectrum for a number of different beam energies and comparing the measured and predicted Q_{ggg} peak positions the beam energy at the center of the target was determined to be 87.7 MeV. After considering the energy loss in the target the energy from the LINAC was found to be 88.5 MeV. For the $^{10}\text{Be}(^{14}\text{C},\alpha\ ^6\text{He})^{14}\text{C}$ reaction $Q_3 = -7.41$ MeV. The Q_{ggg} peak therefore appears at $E_{\text{tot}} = 80.28$ MeV. The peak labeled $Q_{\text{gg}(1)}$, at $E_{\text{tot}} = 73.42$ MeV, is 6.86 MeV lower than the Q_{ggg} peak. These

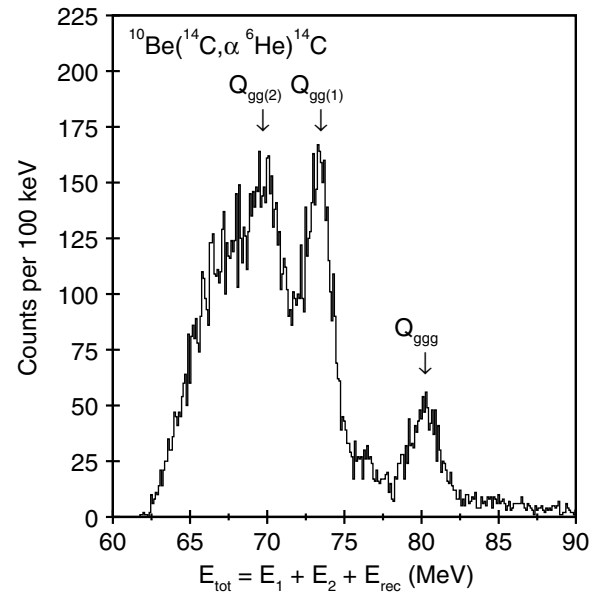


FIG. 2. E_{tot} spectrum for the $^{10}\text{Be}(^{14}\text{C},\alpha\ ^6\text{He})^{14}\text{C}$ reaction.

events correspond to the $^{10}\text{Be}(^{14}\text{C},\alpha\ ^6\text{He})^{14}\text{C}^*$ reaction, with the ^{14}C recoil excited to the 6.094 MeV 1^- , 6.589 MeV 0^+ , 6.728 MeV 3^- , 7.012 MeV 2^+ or 8.318 MeV 2^+ excited state [7]. There is also evidence for a third peak in Fig. 2, labeled $Q_{\text{gg}(2)}$. This appears at an energy of 69.9 MeV, 10.4 MeV lower than the Q_{ggg} peak. Again this corresponds to the $^{10}\text{Be}(^{14}\text{C},\alpha\ ^6\text{He})^{14}\text{C}^*$ channel, with the $^{14}\text{C}^*$ being excited to the 9.746 MeV 0^+ , 9.801 MeV 3^- , 10.425 MeV 2^+ , 10.449 MeV ≥ 1 , 10.498 MeV (3^-) or 10.736 MeV 4^+ excited state [7].

In order to confirm the peaks seen in the E_{tot} spectrum arise from reactions with the ^{10}Be content of the target, and not the ^{16}O or Pt components, a plot of the recoil energy determined from energy conservation ($E_{\text{rec}} - Q_3 = E_{\text{beam}} - E_1 - E_2$) (in MeV) plotted against that determined from momentum conservation ($E_{\text{rec}} = \mathbf{p}_{\text{rec}}^2/2$) (in MeV, where u is the atomic mass unit) was produced (Fig. 3). As the recoil energy is correctly given by $E_{\text{rec}} = \mathbf{p}_{\text{rec}}^2/2m_{\text{rec}}Q_{\text{ggg}}$ events will appear in the spectrum as a locus with a slope given by $1/m_{\text{rec}}$ and an intercept on the $E_{\text{rec}} - Q_3$ axis equal to $-Q_3$. In Fig. 3 the Q_{ggg} events from the $^{10}\text{Be}(^{14}\text{C},\alpha\ ^6\text{He})^{14}\text{C}$ reaction lie on a line with a slope of $1/14$ and an intercept equal to $-Q_3 = 7.41$ MeV. The solid line indicates the predicted location of these events. The dashed line indicates events from the $^{10}\text{Be}(^{14}\text{C},\alpha\ ^6\text{He})^{14}\text{C}^*$ reaction, where the ^{14}C recoil has been assumed to be excited to the 6.589 MeV 0^+ state. The slope is again $1/14$ and the intercept is equal to the sum of $-Q_3$ and the ^{14}C excitation energy. The predicted locus for the $^{16}\text{O}(^{14}\text{C},\alpha\ ^6\text{He})^{20}\text{Ne}$ channel is given by the dotted line. There are a number of possible Pt loci, the most abundant masses being 194, 195, 196 and 198 (32.9, 33.8, 25.3 and 7.2% natural abundance respectively). For clarity only the locus for the $^{195}\text{Pt}(^{14}\text{C},\alpha\ ^6\text{He})^{199}\text{Hg}$ reaction is shown (dot-dash line). The other Pt lines have almost identical slopes and the variation in Q_3 (and hence intercept) is only 1.25 MeV. It is clear from Fig. 3 that the data are best described by the

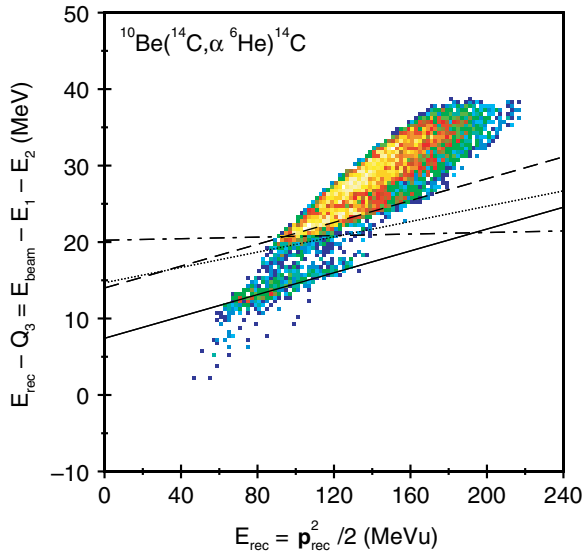


FIG. 3. (Color online) $(E_{\text{rec}} - Q_3)$ vs $\mathbf{p}_{\text{rec}}^2/2$ for the $^{10}\text{Be}(^{14}\text{C}, \alpha \ ^6\text{He})^{14}\text{C}$ reaction. The lines are described in the text. For clarity the data have only been plotted for bins with a content > 2 counts.

loci corresponding to reactions from the ^{10}Be content of the target. This supports the peak identification made for the E_{tot} spectrum shown in Fig. 2.

Total energy spectra were also reconstructed for the $^{10}\text{Be}(^{14}\text{C}, \ ^6\text{He})^{12}\text{C}$ and $^{10}\text{Be}(^{14}\text{C}, \ ^4\text{He})^{12}\text{C}$ reactions. No evidence was seen for a Q_{ggg} peak in either case. These spectra are therefore not shown.

The ^{10}Be excitation energy (E_x) in the $^{10}\text{Be}(^{14}\text{C}, \alpha \ ^6\text{He})^{14}\text{C}$ channel was determined from the relative energy (E_{rel}) between the detected α and ^6He decay products ($E_x = E_{\text{rel}} - Q_2$, where Q_2 is the breakup Q -value) [6]. As the ^{10}Be decay is not affected by any excitation energy carried by the recoiling ^{14}C (as it is produced in the initial $^{10}\text{Be}(^{14}\text{C}, \ ^{10}\text{Be}^*)^{14}\text{C}$ two-body reaction) the E_x spectra for the Q_{ggg} , $Q_{\text{gg}(1)}$ and $Q_{\text{gg}(2)}$ peaks seen in Fig. 2 have been added together. The resultant ^{10}Be E_x spectrum is shown in Fig. 4. The energies of the known [8] states at $E_x = 9.56$, 10.15, 11.23 and 11.76 MeV are indicated. All appear to be observed. The known 10.57 MeV state, however, is very weak (if populated at all). The excitation energies from the present work are compared to the known values in Table I. The dotted line in Fig. 4 indicates the predicted detection efficiency for this

TABLE I. Excitation energies, spins and widths [8] of the states observed in ^{10}Be . The uncertainties quoted in the current work are statistical only. Systematic uncertainties are expected to be 200 keV.

Present work E_x (MeV)	E_x (MeV)	Ref. [8] J^π	$\Gamma_{\text{c.m.}}$ (keV)
9.60 ± 0.01	9.56 ± 0.02	2^+	141 ± 10
10.23 ± 0.01	10.15 ± 0.02	3^-	296 ± 15
	10.57 ± 0.03	≥ 1	
11.00 ± 0.02	11.23 ± 0.05		200 ± 80
11.80 ± 0.02	11.76 ± 0.02	(4^+)	121 ± 10

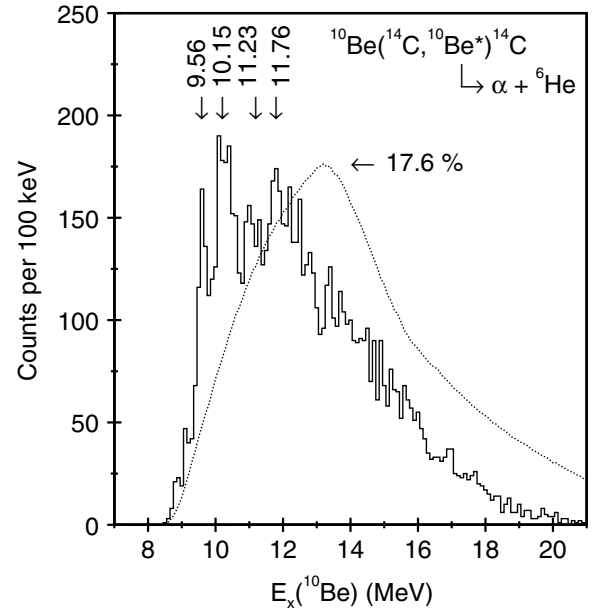


FIG. 4. E_x spectrum for the $\alpha + \ ^6\text{He}$ decay of ^{10}Be .

channel. This was obtained from a Monte Carlo simulation of the reaction and detection system and assumed an exponential angular distribution for the initial $^{10}\text{Be}(^{14}\text{C}, \ ^{10}\text{Be}^*)^{14}\text{C}$ reaction and an isotropic c.m. decay. The peak detection efficiency is indicated (17.6%).

The cross section for the $^{10}\text{Be}(^{14}\text{C}, \alpha \ ^6\text{He})^{14}\text{C}$ reaction, obtained by integrating over all excitations in ^{10}Be , is $(48.4 \pm 5.4) \mu\text{b}$. For the $^6\text{He} + \ ^6\text{He}$ and $^4\text{He} + \ ^8\text{He}$ decay of ^{12}Be the upper limits are 50 and 300, nb respectively. These values are dependent, however, on the angular distributions used in the Monte Carlo simulations of detection efficiency noted above. In the ^{10}Be decay, for example, a factor of two decrease in the exponential angular distribution width, $P(\theta^*) \propto \exp(-\theta^*/16)$, reduces σ by 30%. A factor of two increase in the width results in a 60% increase in the cross-section.

Transfer reactions offer an insight into the structure of the states of ^{10}Be . The work of the group at the Hahn Meitner Institut (Berlin) on pick-up and stripping reactions populating states in ^{10}Be has led to an understanding of their single-particle configurations [9]. For example, the $^9\text{Be}(^{14}\text{N}, \ ^{13}\text{N})^{10}\text{Be}$ reaction strongly populates the states above 9 MeV, at 9.27 MeV (4^-), 11.8 MeV and 15.34 MeV. From rotational systematics it is assumed that the 11.8 and 15.34 MeV states are the 5^- and 6^- members, respectively, of the negative parity band which includes the 9.27 MeV (4^-) state. The neutron transfer reaction would populate two-neutron configurations which include the $p_{3/2}$ orbit of the valence neutron in ^9Be . The negative parity states would then correspond to $p_{3/2} \otimes d_{5/2}$ configurations. The coupling of these orbits would in principle lead to the population of states up to $J^\pi = 4^-$, and higher spin states require angular momentum to be generated from the ^8Be core. It should be noted that the proposed rotational band with member states at 6.18 MeV 0_2^+ , 7.54 MeV 2^+ and 10.15 MeV 4^+ [10], based on a proposed $(sd)^2$ neutron configuration, is not observed as expected. The $2p$ -stripping reaction $^{12}\text{C}(^{15}\text{N}, \ ^{17}\text{F})^{10}\text{Be}$ [9] populates the 9.27 (4^-),

9.56 2^+ , 10.56 and 11.8 MeV states. The two proton removal reaction proceeds in two steps, allowing the excitation of neutron (or proton) particle-hole configurations, which is the explanation for the population of the 9.27 MeV state. The population of the 9.56 MeV and 10.56 MeV states, not observed in the $1n$ -transfer, indicates that these have a more complex configuration than excitations within the p -shell or $1p - 1h$ excitations to the sd -shell. The 9.56 MeV state is strongly populated in the reaction ${}^7\text{Li}({}^7\text{Li}, \alpha {}^6\text{He})\alpha$ [11] as is the 10.15 MeV state, and the 11.8 MeV state to a much lesser extent. The 9.56 and 10.15 MeV states may thus correspond to combinations of one proton and two neutrons in the sd -shell. The present understanding is that the 10.15 MeV state is associated with two neutrons in the sd -shell and thus the additional transferred proton would reside in the p -shell. The 9.65 MeV state may thus correspond to a proton+neutron pair in the sd -shell.

The reaction kinematics and coincident detection of the ${}^4\text{He}$ and ${}^6\text{He}$ at forward angles and high energy in the present ${}^{10}\text{Be}({}^{14}\text{C}, \alpha {}^6\text{He}){}^{14}\text{C}$ reaction indicates the states in ${}^{10}\text{Be}$ are populated following the removal of an α -particle from the ${}^{14}\text{C}$ projectile (and not by a direct decay of the ${}^{10}\text{Be}$ target). Among the states mentioned above the 9.56, 10.15 and 11.8 MeV states are observed. The removal of an α -particle from the dominantly p -shell nucleus ${}^{14}\text{C}$ would, for a single-step process, be expected to produce configurations in ${}^{10}\text{Be}$ in which all the nucleons are confined to the p -shell. Given

the likely configurations of the states populated, it is clear that the present reaction is more complex. It is likely that the contribution of purely p -shell contributions to the excitation energy region above 9 MeV is small, which would explain the small cross section for the present measurements— $(48.4 \pm 5.4) \mu\text{b}$ for *all states* in ${}^{10}\text{Be}$. Similarly, the $2p$ removal from ${}^{14}\text{C}$ populating states in ${}^{12}\text{Be}$ which then decay to ${}^6\text{He} + {}^6\text{He}$ is suppressed, as these states have also been predicted to contain significant sd -shell components [12]. In the present measurements we conclude that neither the higher order components in the ${}^{14}\text{C}$ ground state wave-function, nor the complexity of the reaction process are sufficient to excite the required configurations.

In summary, the ${}^{10}\text{Be}({}^{14}\text{C}, {}^{12}\text{Be}^*){}^{12}\text{C}$ reaction has been used at 88.5 MeV to study the ${}^6\text{He} + {}^6\text{He}$ and $\alpha + {}^8\text{He}$ decay of the molecular rotational band in ${}^{12}\text{Be}$. No evidence for the breakup of ${}^{12}\text{Be}$ was obtained. The upper limits for the cross sections for the ${}^{10}\text{Be}({}^{14}\text{C}, {}^6\text{He} {}^6\text{He}){}^{12}\text{C}$ and ${}^{10}\text{Be}({}^{14}\text{C}, \alpha {}^8\text{He}){}^{12}\text{C}$ reactions are 50 and 300 nb, respectively. The $\alpha + {}^6\text{He}$ decay of ${}^{10}\text{Be}$ was observed via the ${}^{10}\text{Be}({}^{14}\text{C}, \alpha {}^6\text{He}){}^{14}\text{C}$ reaction with a cross section of $(48.4 \pm 5.4) \mu\text{b}$.

The assistance of the staff at the Florida State University superconducting LINAC facility is gratefully acknowledged. This work was funded by the United Kingdom Engineering and Physical Sciences Research Council and the National Science Foundation.

-
- [1] M. Freer *et al.*, Phys. Rev. Lett. **82**, 1383 (1999).
 [2] M. Freer *et al.*, Phys. Rev. C **63**, 034301 (2001); **64**, 019904(E) (2001).
 [3] A. Saito *et al.*, Prog. Theor. Phys. (Kyoto), Suppl. **146**, 615 (2002).
 [4] A. Saito *et al.*, Nucl. Phys. **A738**, 337 (2004).
 [5] D. R. Goosman, Nucl. Instrum. Methods **116**, 445 (1974).
 [6] N. Curtis *et al.*, Nucl. Instrum. Methods A **351**, 359 (1994).
 [7] F. Ajzenberg-Selove, Nucl. Phys. **A523**, 1 (1991).
 [8] D. R. Tilley *et al.*, Nucl. Phys. **A745**, 155 (2004).
 [9] H. G. Bohlen, *Proceedings International Symposium on Exotic Nuclei*, Baikal Lake (Russia), July 2001, edited by Yu. E. Penionzhkevich and E. A. Cherepanov (World Scientific, Singapore, 2001), p. 453.
 [10] M. Freer *et al.*, Phys. Rev. Lett. **96**, 042501 (2006).
 [11] N. Curtis *et al.*, Phys. Rev. C **64**, 044604 (2001).
 [12] Y. Kanada-En'yo *et al.*, Nucl. Phys. **A738**, 3 (2004).